Volume 2, 2026, Pages 212-224 *Journal of Smart and Sustainable Farming*
| Regular Article | Open Access

Spatiotemporal Modelling of Agricultural Greenhouse Gas Emissions for Sustainable Farm Management

Ketema Niguse Baye
Forestry Department, School of Agriculture and Natural Resource Management, Mattu University, Metu, Ethiopia.
ketema.niguse@mau.edu.et

Tommy Dalgaard
Agrobiotechnology, Agrarian and Technological Institute, RUDN University, Moscow 117198, Russia.
dalgaardtommys@rudn.ru

Article Info
Journal of Smart and Sustainable Farming
https://www.ansispublications.com/jssf/jssf.html

© The Author(s), 2026.
https://doi.org/10.64026/JSSF/2026018

Received 12 May 2026
Revised from 21 August 2026
Accepted 30 August 2026
Available online 22 September 2026
Published by Ansis Publications.

Corresponding author(s):
Tommy Dalgaard, Agrobiotechnology, Agrarian and Technological Institute, RUDN University, Moscow 117198, Russia.
dalgaardtommys@rudn.ru

This article is an open access article distributed under the terms and conditions of the Creative Commons Attribution (CC BY) license (https://creativecommons.org/licenses/by/4.0/).

Abstract – Greenhouse-gas (GHG) emissions from farms are highly variable in space and time: nitrous oxide (N_2O) is released in short bursts after fertilisation and rain on wet soil, methane (CH_4) is emitted from flooded rice, and both differ between parcels. Annual emission factors and a few chamber measurements cannot resolve this variability, which limits farm-level inventories and mitigation planning. This paper develops a spatiotemporal modelling framework for daily, parcel-level N_2O and CH_4 emissions that combines sparse chamber measurements, weather, soil-moisture, management and satellite-vegetation covariates with a process-guided gradient-boosting model, validated under random, spatial, temporal and spatiotemporal splits and upscaled to unsampled parcels with regression kriging. A simulated 144-ha farm with 24 chamber parcels and 3,230 chamber observations over two years was used, in which the true fluxes are known. The simulated farm emitted about 406 t CO_2e per year, of which 67 % was rice methane; a mean N_2O emission factor of 1.0 % was reproduced, and 40 % of annual N_2O was emitted on 10 % of days. The hybrid model explained 27 % of the variance of daily N_2O flux on unseen parcels in an unseen year (59 % on the square-root scale) and 80 % of CH_4, whereas study-blind random splits overstated N_2O accuracy by a factor of 2.1. Upscaled annual CO_2e per parcel reached $R^2 = 0.97$ on unsampled parcels against 0.80 for IPCC Tier 1 factors, although the farm total was underestimated by 5 %. Chamber networks that covered all crops and soil classes gave much smaller farm-total errors than random placement when few parcels were sampled, and scenario analysis showed that water management in rice and nitrification inhibitors dominated mitigation, with N-rate reduction and application timing worth only a few per cent.

Keywords – Greenhouse Gases, Nitrous Oxide, Methane, Spatiotemporal Modelling, Regression Kriging, Mitigation.

I. INTRODUCTION

Background and Research Motivation

It is estimated that agriculture makes large contributions of anthropogenic greenhouse gas (GHG) emissions, mainly from the emission of nitrous oxide (N_2O) from soils receiving nitrogen fertilization; from the emission of methane (CH_4) from flooded rice fields and from livestock farming; and from agricultural energy use and land-use change, which are directly responsible for the emission of carbon dioxide (CO_2) from the air. Agricultural management provides also significant potential for reducing emissions by optimizing nutrient use, water management, and soil conservation. A reliable quantification of these emissions is therefore necessary to develop farm management strategies for sustainability and to assess the effectiveness of mitigation [1].

Standardised emission factors are used in conventional farming GHG inventories. In some cases, the default values for direct N_2O emissions are based on the Intergovernmental Panel on Climate Change (IPCC) Tier 1 method (e.g., 1% of

applied nitrogen as N_2O-N) or the default daily emission factors for rice methane, modified by water management and organic amendment [2]. While these methods can facilitate a consistent development of inventory, the generalised assumptions they make are not fully representative of field level variability. The mineral nitrogen availability, soil moisture, temperature, and carbon availability all have nonlinear interactions that affect N_2O emissions, especially when fertilization and rainfall occur. Likewise, the amount of CH_4 released from rice systems is influenced by the duration of flooding, soil temperature, amount of organic carbon, and irrigation methods [3].

Such processes result in strong variations in the emission not only from one period to another, but also in space, with emission hotspots and emission peaks of short duration. These events are often referred to as 'hotspots' or 'hot moments' and can make a significant contribution to annual emissions. Although important biogeochemical processes, process-based models such as DNDC and NOE models are very data and parameter intensive and require high computational power. Moreover, their capability to emit short pulses is still a function of the input quality and the model structure. Closed-chamber measurements allow direct measurement of fluxes but are labor intensive, usually resulting in limited samples and area coverage, which means they may also miss important emission events and may not adequately capture farm-wide variability [4].

Research Challenges

The opportunities to model complex relationships between GHG emissions and environmental drivers become apparent when combining chamber measurements with information from meteorological, soil, management and satellite-derived data, and machine-learning techniques. But there are three big problems yet to be solved. First, high spatial and temporal autocorrelations can lead to overoptimistic predictive results if one sets a random partition of the training and test sets. Second, models that are developed from a small number of monitored parcels should be able to generalize to fields not sampled and years not covered [5]. Third, predictions need to be interpreted in terms of space-specific emission estimates, inventories at the farm scale, comparisons that take into account uncertainty, and specific management recommendations [6].

To overcome these difficulties, the present study presents a process-based approach to modelling N_2O and CH_4 emissions with spatial and temporal resolution on a daily and parcel basis. This framework combines the output of the process-models with environmental and management covariates in a gradient-boosting regression model. It is compared to linear regression, process only modelling, random forest and conventional boosting techniques, and validated by random, spatial, temporal and spatiotemporal validation methods. The residual is then modeled as a spatial process and regression kriging is used to estimate emissions at unmonitored parcels and take into account the spatially correlated residual, before comparing the annual emission inventories to Tier 1 estimates produced by the IPCC [7].

The study also explores the various types of chamber-network placement strategies (random, stratified, covariate-balanced sampling) and examines the effect of the monitoring design on the estimation errors on the farm total. Management scenarios include the examination of the level of nitrogen application, fertilizer splitting and timing, nitrification inhibitors, and rice water management. Comprehensive daily flux observations are not often available for complete farms; therefore, a simulated 144-ha agricultural system, with known underlying emissions is employed to assess model performance against ground truth. This controlled experimental design allows to evaluate systematically the predictive transferability, spatial upscaling, monitoring efficiency, and mitigation potential, which can help to inform more confident data-informed management decisions for sustainable farms [8].

This paper is organized as follows: The review of existing literature is presented in section 2, covering the modelling of agricultural GHG, process-based methods, machine learning and spatial upscaling. In Section 3, the proposed spatiotemporal modelling framework is presented, consisting of model development, validation strategies, regression kriging and management scenario analysis. The experimental results, predictive performance, spatial emission patterns, design of monitoring networks, and mitigation potential are discussed in Section 4. Lastly, Section 5 provides an overview of the major findings, contribution, limitations and future research directions.

II. LITERATURE REVIEW

GHG emission modelling for agriculture has progressed from a single-purpose, standardized method of calculating emissions based on emission factors to a more flexible method that incorporates spatial and temporal heterogeneity and farm management practices. Traditional inventory approaches account for the emissions of nitrous oxide (N_2O) mainly as a function of inputs of nitrogen and of methane (CH_4) emissions from rice production by applying known emission factors. While these techniques can be used for national inventories and large scale reporting, they are not readily applicable for reporting at the parcel level, due to the assumption of similar emission rates between fields and growing season. The differences in soil properties, irrigation regimes, crop characteristics, fertiliser application and weather conditions can lead to significant differences that cannot be captured by annual averages. Thus, better modelling methods to describe the temporal variation of emissions and enable spatial planning for mitigation measures are needed [9].

Process based biogeochemical models will serve as a basis to represent the processes and mechanisms that regulate agricultural GHG emissions. These models simulate nitrogen transformation as well as degradation of soil organic matter, microbial activity, soil water movement, and crop development in order to predict the fluxes of emissions as environmental conditions change. Nitrification, denitrification, soil oxygen and soil nitrogen availability-moisture interactions are

important factors on N_2O emissions. The production and transport of CH_4 relies on anaerobic conditions, soil temperature, organic carbon availability and water management, in flooded rice systems. Although process-based models have several advantages over a mechanistic approach, they require a detailed parameterization and input data that may not be available for each parcel. They may also be further complicated by the uncertainty of parameters and computational needs in application to heterogenous farms [10].

Machine-learning techniques can provide an alternative approach for data collection of non-linear relationships between the environmental drivers and observed emission fluxes. Tree-based ensemble algorithms such as random forests and gradient boosting do not need to specify all the underlying processes and can incorporate meteorological data, soil properties, crop data, management data, and remotely sensed vegetation data. The methods are well suited to detecting emission peaks after rain and after fertilization and to differentiating the contrasting responses of crop and soil classes. But if the data available for training are limited or the environment differs from the one in which the model was developed, strictly empirical models can make physically implausible predictions. Features, constraints on management, and biologically meaningful transformations informed by processes can enhance the interpretability and robustness of data-driven predictions [11].

The use of remote sensing and geographic information systems has increased the possibilities to monitor spatial and temporal agriculture variability. Field observations are complemented with information derived from satellites on the vegetation indices, land cover and crop growth indicators on a spatial extent. In conjunction with weather information, soil moisture estimates, and management information, these covariates can be used to describe the difference between monitored and unmonitored parcels for use in emission models. However, the satellite-based measurements cannot observe soil GHG fluxes directly and short-lived events of GHG flux can be masked by cloud cover, observation frequency, and the limited temporal resolution. Sparse chamber measurements are thus still valuable for the calibration and assessment of predictive models [12].

Besides the emissions measured at monitoring locations, spatial interpolation methods, especially kriging and regression kriging, offer further possibilities for mapping emissions. The predictions from the environmental covariates are supplemented by spatially correlated residuals this can improve the parcel-level prediction where there is limited measurement data available regression kriging. The cross-validation technique with randomly partitioned observations, however, can introduce an error in the estimated predictive performance by having similar observations or samples from the same parcels in the training and testing sets. Spatial, temporal, and combined spatiotemporal validation is thus crucial to evaluate the transferability to new locations and years [13].

An integrated framework that integrates process-guided machine learning, sparse chamber observations, multiscale environmental covariates, thorough transferability evaluation, and spatial upscaling is significant for farm-level GHG management despite these advances. The proposed study will aim to fill this gap by simultaneously modelling daily N_2O and CH_4 emissions, testing various validation strategies, using regression kriging to estimate these fluxes for unsampled parcels, and comparing the performance of different monitoring network designs and mitigation scenarios. The integration should strive to enhance the accuracy of the spatial representation of emissions inventories and deliver verifiable information for sustainable use of farms [14].

III. PROPOSED METHODOLOGY

The framework shown in **Fig. 1** has six steps: sensing (chambers, weather, soil-moisture and satellite-vegetation data), process-guided modelling, spatiotemporal validation, upscaling to daily maps and totals, design of the measurement network, and use of the model for management scenarios.

Simulated Farm and Emission Processes

The study farm consists of 144 one-hectare parcels (12 × 12) over two calendar years (730 days) in a tropical monsoon climate. Three cropping systems occupy contiguous blocks (**Table 1, Fig. 2**): flooded rice in 60 parcels (kharif season only, with fallow in the rabi season), maize in 48 parcels and vegetables in 36 parcels (both seasons). Soil organic carbon, pH and sand content are spatially correlated fields, 64 parcels are poorly drained, and a latent spatially correlated factor, which is not available to the models, multiplies the N_2O emission to represent unmeasured hot spots. Daily weather was generated with seasonal temperature and a monsoon rainfall pattern. The topsoil water-filled pore space (WFPS) follows a simple water balance with irrigation of maize and vegetables below a threshold and permanent flooding of rice for 110 days after transplanting. Mineral nitrogen in the soil, N, is increased by fertiliser applications A_t and mineralisation m and decays by crop uptake and losses at a rate k_t that is higher during the crop season,

$$N_t = N_{t-1} e^{-k}{}_t + A_t + m \quad (1)$$

The daily N_2O flux (g N ha^{-1} d^{-1}) is the product of functions of mineral nitrogen, temperature and WFPS, modified by soil properties, crop, the latent hot-spot factor and a post-fertilisation rain pulse, with multiplicative log-normal noise (σ = 0.6),

$$F_{N2O} = \left[c \frac{N_t}{N_t+60} 2^{(T-25)/10} \exp\left(-\left(\frac{W-0.75}{0.17}\right)^2\right) f_{soil} f_{crop} L \cdot \pi\right] + F_{bg}, \quad \pi = 1 + 4 \cdot 1[\text{rain} > 20\ \text{mm}, \leq 12\ \text{d after fertiliser}] \quad (2)$$

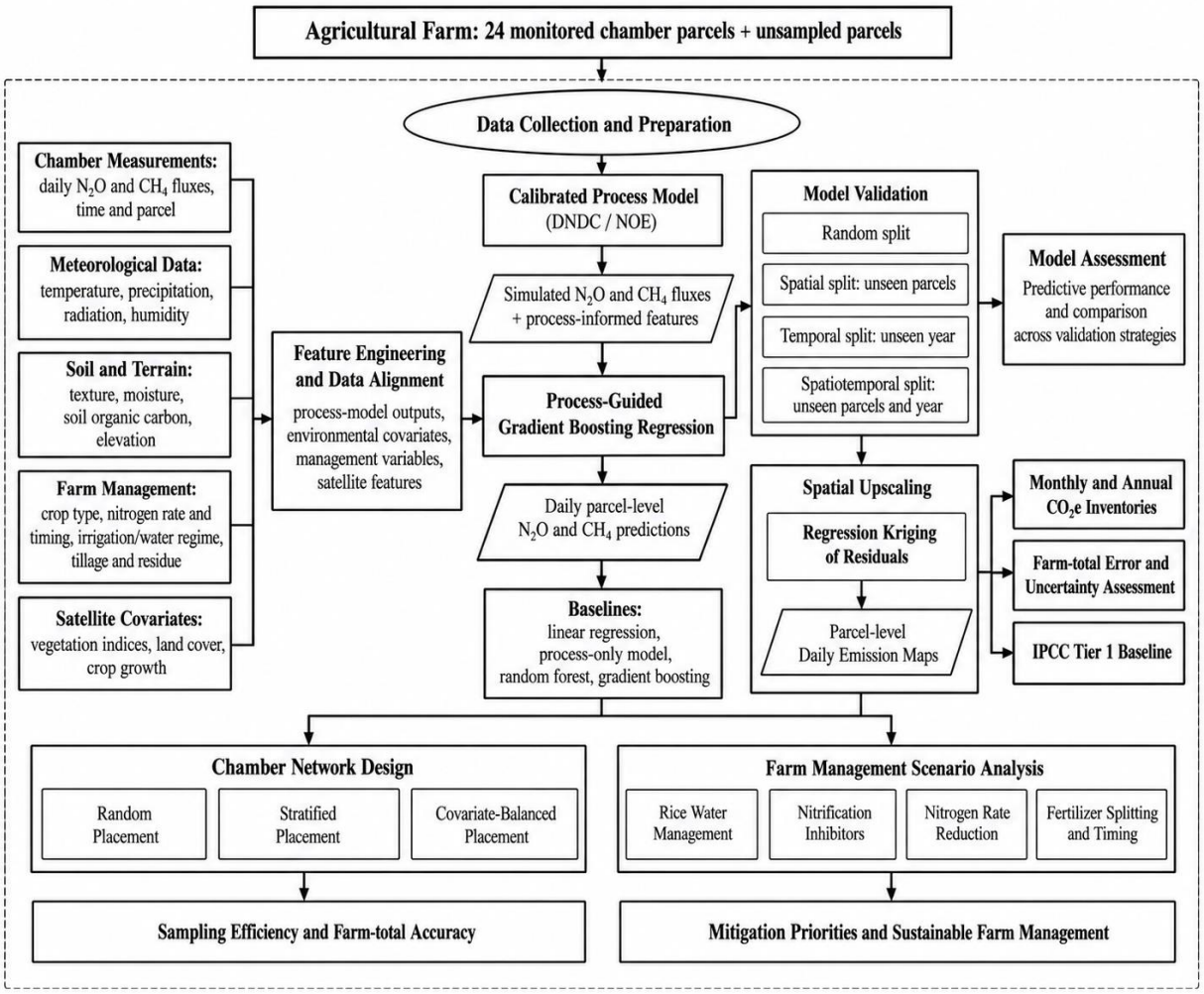


Fig 1. Framework for Spatiotemporal Modelling of Agricultural GHG Emissions for Farm Management.

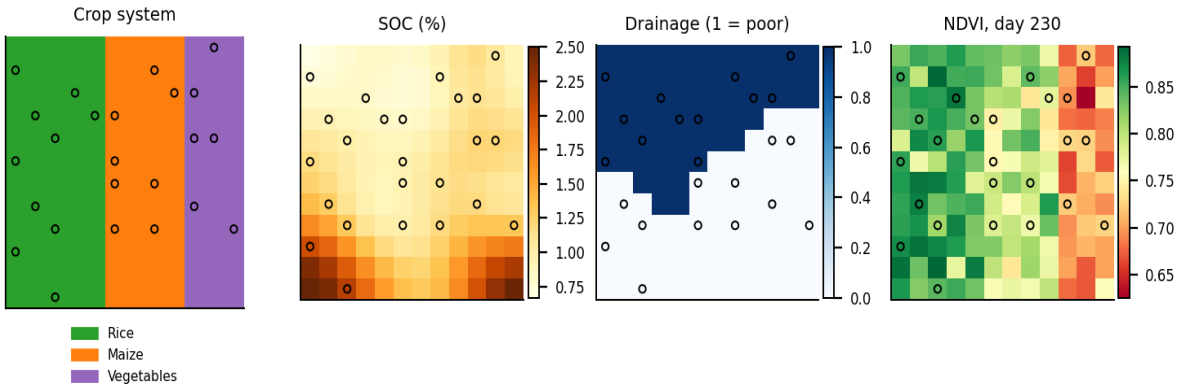


Fig 2. Simulated Farm: Crop Blocks, Soil Organic Carbon, Drainage and Satellite NDVI on Day 230. Circles Mark the 24 Chamber Parcels.

where W is WFPS, L the latent spatial factor and c a constant calibrated so that the mean annual emission factor is about 1 % of the applied N, consistent with the IPCC Tier 1 default [2]. Rice methane occurs only while the field is flooded, with a rate that increases with soil organic carbon and temperature and follows a seasonal curve $\rho(t)$,

$$\mathrm{F_{CH4}} = \mathrm{r_0}\left(\frac{\mathrm{SOC}}{1.2}\right)^{0.6} 1.12^{\mathrm{T}-27}\rho(\mathrm{t})\cdot\varepsilon, \quad \mathrm{r_0} \approx 1.0\ \mathrm{kg\ CH_4\ ha^{-1}\ d^{-1}} \tag{3}$$

Fluxes are expressed as CO_2e with the 100-year global warming potentials of 273 for N_2O and 27 for CH_4,

$$\mathrm{E_{CO2e}} = \mathrm{GWP_{N2O}}\cdot\mathrm{E_{N2O-N}}\cdot\frac{44}{28} + \mathrm{GWP_{CH4}}\cdot\mathrm{E_{CH4}} \tag{4}$$

and the IPCC Tier 1 estimate of N_2O is simply $E_{N2O\text{-}N} = EF \cdot N_{in}$ with $EF = 0.01$. These generating mechanisms are assumptions chosen to reproduce the known qualitative behaviour of N_2O and CH_4, such as hot moments after fertilisation and rain on wet soil [6,7], not parameters of a particular soil. The nitrogen management of the three crops is summarised in **Table 1**; the application dates vary by ±4 days among parcels.

Table 1. Cropping Systems and Baseline Nitrogen Management of the Simulated Farm

Crop	Parcels	Seasons per year	N per season (kg/ha)	Baseline splits
Rice (flooded)	60	1 (kharif)	120	3 (40/30/30%)
Maize	48	2 (kharif, rabi)	150 / 120	2 (40/60%)
Vegetables	36	2 (kharif, rabi)	180	3 (30/35/35%)
Wheat	30	1 (rabi)	120	3 (50/25/25%)
Sorghum	24	2 (kharif, rabi)	80 / 60	2 (50/50%)
Groundnut	24	1 (kharif)	25	2 (50/50%)
Soybean	24	1 (kharif)	30	2 (50/50%)
Cotton	30	1 (kharif)	120	3 (40/30/30%)
Sugarcane	18	1 (annual)	250	4 (25/25/25/25%)
Millet (pearl/finger)	24	1 (kharif)	60	2 (50/50%)
Pulses (chickpea)	18	1 (rabi)	25	1 (100%)
Potato	18	2 (kharif, rabi)	150	3 (25/50/25%)
Onion	18	2 (kharif, rabi)	120	3 (30/40/30%)
Banana	12	Multiple growth cycles	200	4 (25/25/25/25%)
Total	384	—	—	—

Chamber Measurements and Covariates

Chambers were placed on 24 parcels (10 rice, 8 maize and 6 vegetable parcels) chosen at random within crops. Each parcel was sampled once a week, with additional samples two and five days after each fertilisation and one day after rainfall above 25 mm, a common event-based supplement to routine sampling [11], giving 3,230 observations of N_2O and CH_4 fluxes, with a 15 % log-normal measurement error. The covariates available to the models for any parcel and day were weather (temperature and its 3-day mean, rainfall today and over 3 and 7 days, seasonal harmonics), measured WFPS and its lag (a soil-moisture sensor or radar proxy with 0.04 error), nitrogen management (days since the last application and the N applied in the last 14 days), crop and canopy greenness (NDVI from satellite time series), soil properties (SOC, pH, sand, drainage) and, for rice, the flooding state and days since flooding. Parcel coordinates were deliberately excluded from the main models.

Models

Five models of daily N_2O flux were compared: ridge regression; a process model with the structure of the N_2O flux function (a saturating response to mineral nitrogen, a Q_{10} temperature response and a Gaussian response to WFPS) whose parameters were fitted to the chamber data, with mineral nitrogen estimated from the application schedule for a grid of decay rates,

$$\mathrm{F_{proc}} = \mathrm{a}\frac{\hat{\mathrm{N}}_\mathrm{t}}{\hat{\mathrm{N}}_\mathrm{t}+\mathrm{K}}2^{(\mathrm{T}-25)/10}\exp\left(-\left(\frac{\mathrm{W}-\mathrm{w_0}}{\mathrm{s}}\right)^2\right) + \mathrm{b} \tag{5}$$

a random forest; gradient-boosted trees [13], which build an additive model $F_m = F_{m-1} + \nu h_m$; and a hybrid model, a gradient-boosting regressor that receives the process-model output as an additional feature, a simple form of process-guided machine learning in the spirit of hybrid modelling [12]. For CH_4 (flooded rice only), ridge, random forest and boosting models were used. Fluxes are right-skewed, so the models were trained on the square root of the flux and back-transformed with a variance correction to retain unbiased totals,

$$\mathrm{F} = \hat{\mathrm{s}}^2 + {\sigma_\mathrm{e}}^2, \quad \hat{\mathrm{s}} = \max\left(0, \text{model output on } \sqrt{\mathrm{F}}\right) \tag{6}$$

Validation

Four validation schemes were applied to the chamber observations, in line with recommendations for data with spatial and temporal structure [14,15]: (i) random folds, which are expected to be optimistic because neighbouring days of the same parcel appear in both the training and test sets; (ii) spatial folds, in which all observations of four chamber parcels (stratified by crop) are held out; (iii) a temporal split, with training on year 1 and testing on year 2; and (iv) a spatiotemporal split, with training on year 1 and parcels outside a fold and testing on the held-out parcels in year 2. The process model was refitted within every fold. Performance was summarised by the coefficient of determination of daily flux (the primary metric, which is sensitive to hot moments), the R^2 on the square-root scale and the relative error of the cumulative flux,

$$R^2 = 1 - \frac{\sum_i (y_i - \hat{y}_i)^2}{\sum_i (y_i - \bar{y})^2}, \quad \delta_{cum} = \frac{\sum_i \hat{y}_i}{\sum_i y_i} - 1 \tag{7}$$

The importance of groups of predictors was obtained by permuting the columns of a group in the held-out fold and measuring the increase in the root-mean-square error on the square-root scale.

Upscaling, Kriging and Hot Spots

The final models were trained on all chamber data and used to predict the daily fluxes of all 144 parcels, from which annual, monthly and farm totals were derived; the truth is known for all parcels, so the accuracy was evaluated on the 120 parcels without chambers. The IPCC Tier 1 estimate served as a benchmark. Residuals of the model at the chamber parcels, defined as the difference between the annual emission obtained by linear interpolation of the chamber time series (a standard practice for annual chamber estimates) and the model, were interpolated by Gaussian-process regression with a Matérn kernel, a form of regression kriging [16,17],

$$\hat{z}(s_0) = \hat{m}(s_0) + \sum_{i=1}^{n} \lambda_i e(s_i), \gamma(h) = c_0 + c_1\left(1 - e^{-3h/a}\right) \tag{8}$$

where $\hat{m}$ is the model prediction (the trend), e the residual at sampled parcel s_i, λ_i the kriging weights and $\gamma(h)$ an exponential semivariogram with nugget c_0, partial sill c_1 and range a, which was also used to describe the spatial structure of the emissions. Concentration of emissions in time and space was measured by the share of annual emissions that comes from the top fraction q of days or parcels,

$$S(q) = \frac{\sum_{i=1}^{\lceil qn \rceil} F_{(i)}}{\sum_{i=1}^{n} F_{(i)}}, \quad F_{(1)} \geq F_{(2)} \geq \tag{9}$$

Measurement-Network Design and Management Scenarios

To study where to measure, chamber networks of 6, 12, 24 and 48 parcels were selected by three designs: random; stratified by crop and drainage class; and covariate-balanced, in which the parcels nearest to the centres of k-means clusters of coordinates, soil properties, drainage and crop were chosen. For each design and size, five networks were sampled with the same protocol, a model was trained and the farm-total CO_2e for the two years was compared with the truth. For management analysis, seven scenarios were simulated with the same weather and noise: a 20 % lower N rate; more split doses; forecast-guided timing (application delayed up to five days when more than 15 mm of rain is expected within three days); a nitrification inhibitor (N_2O multiplied by 0.6, an assumed effect); alternate wetting and drying (AWD) in rice (CH_4 multiplied by 0.52 as in IPCC scaling factors, with N_2O increased by 25 %, an assumption); and a combined package. For the first three scenarios the data-driven model, fed with the new management and the resulting soil-moisture and weather covariates, predicted the change, which tests whether a model trained on baseline data can support counterfactual use; the inhibitor and AWD effects were applied as external multipliers to both truth and model. Yield was calculated with a quadratic-plateau response to N with assumed small yield bonuses for splitting (+2 %) and timing (+1.5 %), and the yield-scaled emission was $YSE = E_{CO2e} / Y$.

IV. RESULTS AND DISCUSSION

Spatial and Temporal Structure of Emissions

The simulated farm emitted 406 t CO_2e in year 1 and 419 t in year 2, with a mean N_2O emission factor of 0.97 % of the applied N in year 1. Rice dominated the farm total, at 4.9 t CO_2e per hectare and year, almost all of it methane (171 kg CH_4 ha^{-1} yr^{-1}); maize and vegetables emitted 0.9 and 1.9 t CO_2e per hectare, but their N_2O emissions per hectare (2.1 and 4.7 kg N_2O-N) were far higher than those of rice (0.7 kg). **Fig. 3** illustrates the temporal pattern for a maize parcel: after each fertiliser application the flux rises when rain wets the soil towards the optimum WFPS, and between events it falls back to a background level. These are the hot moments (**Fig. 4a**): 40 % of the annual N_2O of the farm was emitted on 10 % of the days, and the 5 % highest parcel-days accounted for 44 % of the annual emission. The concentration in space was lower: the 10 % highest-emitting parcels emitted 24 % of the farm's N_2O, and 23 % of its CO_2e. The farm-level N_2O series had a lag-1 autocorrelation of 0.42 and a lag-7 autocorrelation of 0.25 (**Fig. 4b**), so that weekly sampling captures part of the temporal pattern but misses many pulses. The semivariogram of annual N_2O after removal of the crop effect (**Fig. 4c**) had

a nugget close to zero and a range of 3.7 parcels, which defines the distance over which a chamber parcel is informative about its neighbours and justifies the kriging of residuals.

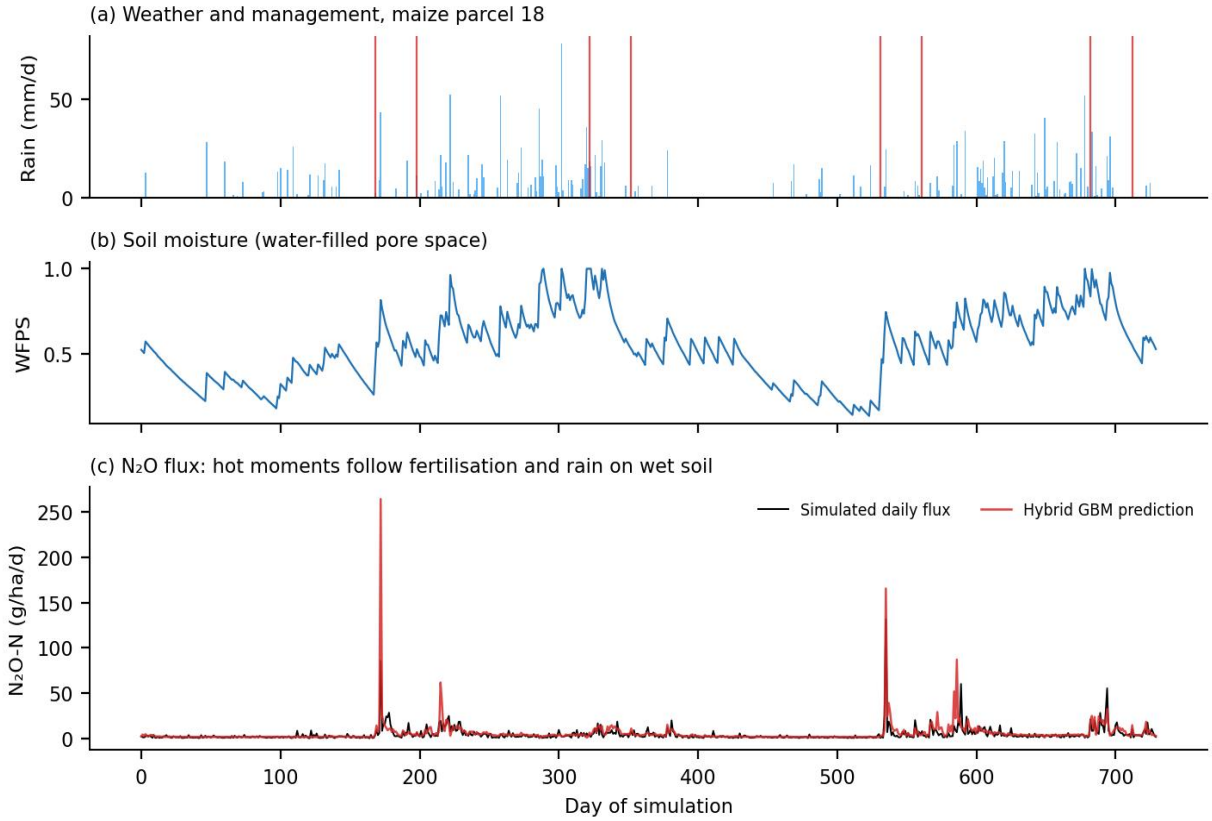


Fig 3. Daily Rainfall and Fertiliser Events (Red Lines), Water-Filled Pore Space and N_2O Flux of One Maize Parcel: Simulated Truth, Hybrid-Model Prediction and Chamber Observations.

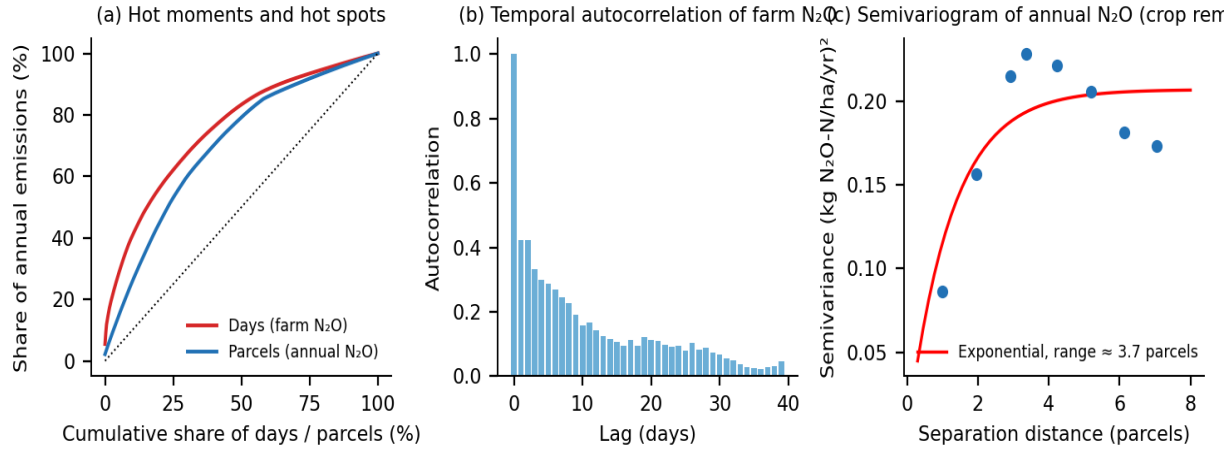


Fig 4. (a) Concentration of N_2O Emissions in Days and Parcels, (b) Temporal Autocorrelation of The Farm N_2O Flux and (c) Semivariogram of Annual N_2O After Removing the Crop Effect, With an Exponential Fit.

Model Comparison Under Spatiotemporal Validation

Table 2 and **Fig. 5** show the performance of the models. For N_2O, the hybrid model was the best under all schemes, followed by boosting, the random forest, the process-only model and ridge regression. Under the strictest, spatiotemporal scheme, the hybrid model explained 27 % of the variance of daily flux (59 % on the square-root scale), against 23 % for boosting alone, 16 % for the process model and 10 % for ridge regression. The advantage of the hybrid over boosting was small in absolute terms (4 percentage points) but consistent across schemes, which indicates that the process model supplies a useful, physically meaningful feature when data are few. The absolute accuracy is modest, as expected for a flux with a noise level of 60 % and hot moments of a few days; much of the variance is irreducible. The pattern across validation

schemes is the most important result: random folds gave $R^2 = 0.57$ for the hybrid, spatial folds 0.45, the temporal split 0.32 and the spatiotemporal split 0.27. Random folds overstate the accuracy for new parcels and years by a factor of 2.1, since neighbouring days of a parcel share the unmeasured latent hot-spot factor and management, so that the model recognises the parcel. A model that is to be used for unmeasured parcels and future seasons must be judged under spatiotemporal validation [14,15]. The cumulative flux of the held-out observations was biased by -31 % in the spatiotemporal scheme (negative values mean underestimation), which is carried into the totals below.

Methane was much easier to predict, since it is controlled by the flooding state, temperature, season and soil carbon: the random forest reached $R^2 = 0.80$ in the spatiotemporal scheme, with little difference between schemes (0.83 to 0.80) and ridge regression only slightly lower (0.78), which shows that the CH_4 signal is smooth and largely additive in the covariates while N_2O is dominated by interactions.

Table 2. Coefficient of Determination of Daily N_2O Flux and of CH_4 in Rice

Model	Random	Spatial	Temporal	Spatiotemporal	Spatiotemp. (√)
N_2O: Ridge	0.16	0.15	0.10	0.10	0.38
N_2O: Process model	0.21	0.21	0.16	0.16	0.50
N_2O: Random Forest	0.50	0.39	0.26	0.21	0.57
N_2O: Gradient boosting	0.53	0.44	0.29	0.23	0.56
N_2O: Hybrid GBM	0.57	0.45	0.32	0.27	0.59
CH_4: Ridge	0.80	0.79	0.78	0.78	0.92
CH_4: Random Forest	0.83	0.81	0.82	0.80	0.94
CH_4: Gradient boosting	0.81	0.78	0.82	0.79	0.94

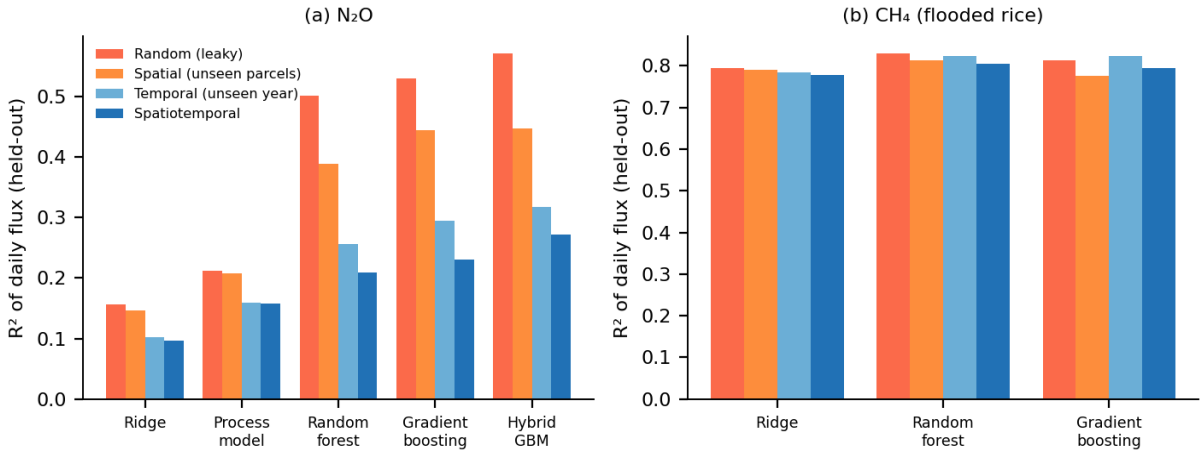


Fig 5. Daily-Flux R^2 of the Models Under Four Validation Schemes for (A) N_2O and (B) CH_4.

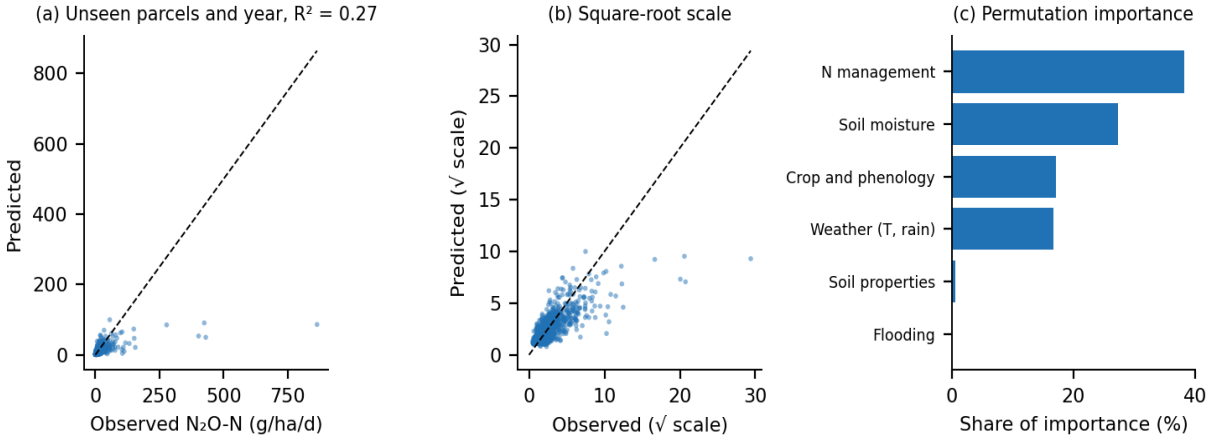


Fig 6. Hybrid Model Under Spatiotemporal Validation: (A) Predicted Versus Observed Daily N_2O Flux, (B) The Same on a Square-Root Scale and (C) Permutation Importance of Predictor Groups.

Fig. 6 shows predicted against observed fluxes for unseen parcels and the following year, and the importance of groups of predictors. Predictions follow the observations but compress the highest values, which explains the underestimation of

the totals. The most important predictors were n management (38 % of the total importance), soil moisture (27 %) and crop and phenology and weather (t, rain) (17 % and 17 %). This agrees with the mechanisms: the flux depends on the nitrogen supplied and its recency, on soil moisture, and on weather and crop stage, whereas soil properties were of little importance in the model (1 %), because in this farm the variation between parcels is carried mainly by crop and by the latent factor, and not by the measured soil properties. This should not be taken to mean that soil properties never matter; in real data with stronger SOC and texture gradients they would be expected to contribute more.

Upscaling to Unsampled Parcels

Table 3 and **Fig. 7** compare annual predictions for the 120 parcels without chambers. For CO_2e, the IPCC Tier 1 estimate, which depends only on crop, nitrogen applied and flooded days, explained 80 % of the variance between parcels, the hybrid model 96 % and the hybrid model with kriged residuals 97 %, with the RMSE falling from 0.86 to 0.37 and 0.31 t CO_2e ha^{-1} yr^{-1}. Because methane dominates the farm total, these figures mainly reflect rice; for N_2O alone, the annual parcel-level R^2 was 0.65 for Tier 1, 0.80 for boosting and 0.85 for the hybrid model. Kriging the residuals improved the CO_2e estimates further and reduced the bias, because part of the error is spatially structured and the nearby chamber parcels carry information on it. The farm totals tell a more cautious story: all methods underestimated the farm CO_2e (-10 % for Tier 1, -8 % for the hybrid and -5 % with kriging), and for N_2O the model underestimated by 11 %, whereas Tier 1 was within 2 % of the total because the simulator was calibrated to its emission factor. The model is thus much better at ranking and mapping parcels than at the absolute total, and the remaining bias, which results from hot moments that are not captured, is a systematic uncertainty that has to be reported with the inventory.

Table 3. Accuracy of Annual Emission Estimates for the 120 Parcels Without Chambers

Method	R^2 (CO_2e)	RMSE (t/ha/yr)	Bias (t/ha/yr)	Farm total error (%)	R^2 (N_2O only)
IPCC Tier 1 [15]	0.800	0.86	-0.31	-10.5	0.65
Gradient boosting [16]	0.957	0.40	-0.28	-8.9	0.80
Hybrid GBM [17]	0.962	0.37	-0.26	-8.3	0.85
Hybrid GBM + kriging	0.974	0.31	-0.17	-5.2	—

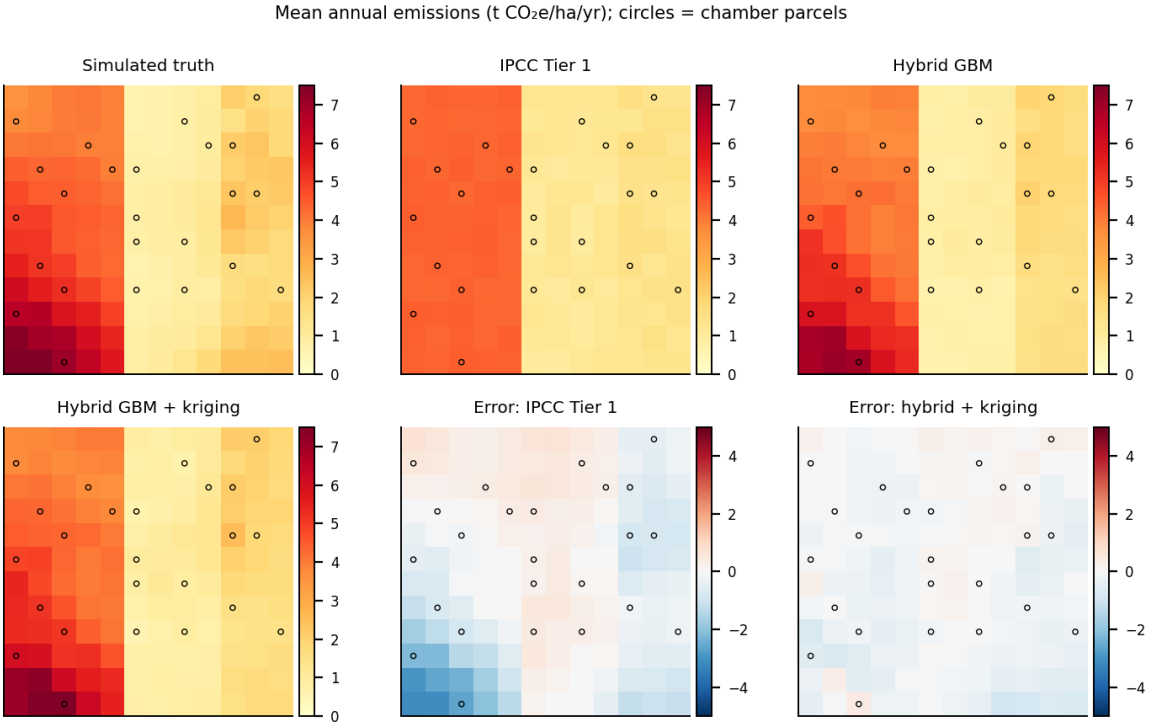


Fig 7. Mean Annual Emissions (T CO_2E/Ha/Yr): Simulated Truth, IPCC Tier 1, Hybrid Model and Hybrid Model with Kriged Residuals (Top), and Errors of Tier 1 and of the Hybrid Model with Kriging (Bottom).

The daily predictions for parcels without chambers explained 48 % of the variance of the daily N_2O flux and 88 % of the variance of the farm-total daily series, and the 5 % highest predicted parcel-days overlapped with the true 5 % highest in 59 % of the cases; the predicted pulses carried 37 % of the annual emissions, compared with 44 % in reality. The monthly maps (**Fig. 8**) reproduced the seasonal pattern, with a peak in the flooding months, and the monthly parcel-level R^2 was 0.98. The space–time view in **Fig. 9**, which averages the flux over rows, shows that the model reproduces the rice block's

emission during the monsoon season and the maize and vegetable pulses after fertilisation, while the intensity of single pulses is smoother in the prediction than in the simulation. These maps are the form in which the results would be used in practice, for identification of the periods and parcels that need attention.

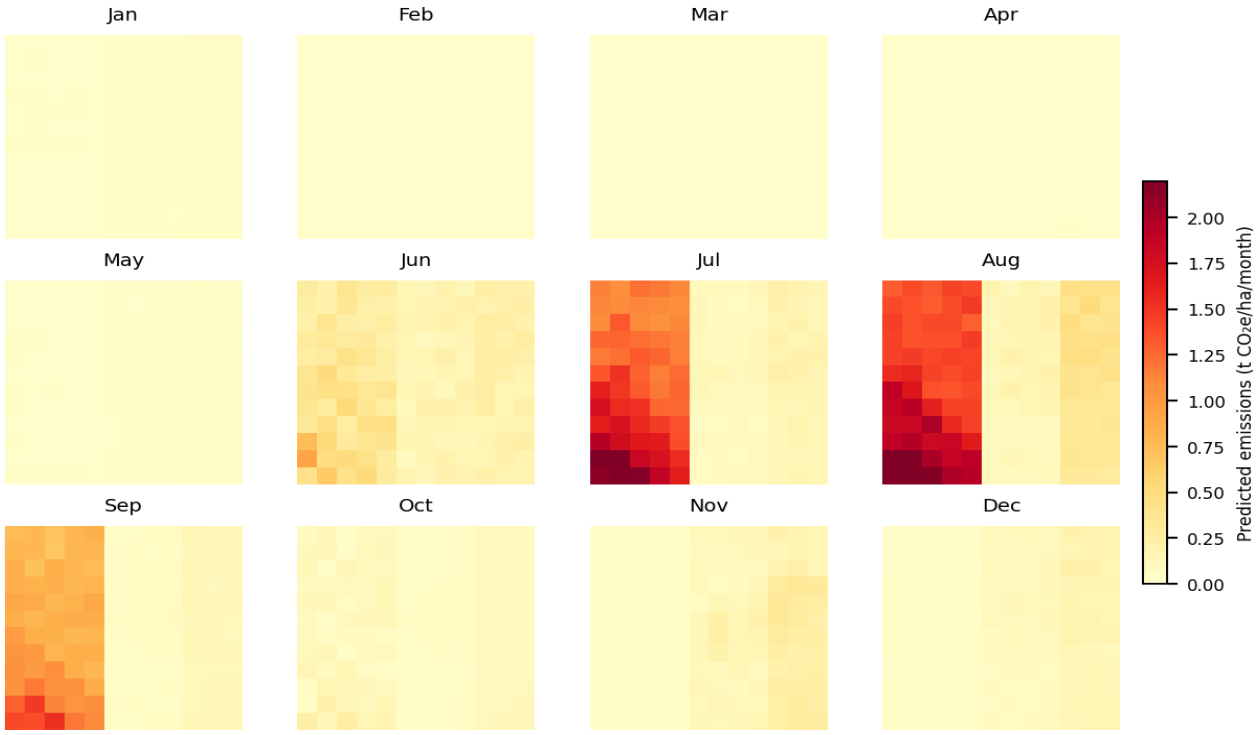


Fig 8. Predicted Monthly Emissions of Year 1 (T CO_2E/Ha/Month) From the Hybrid Model.

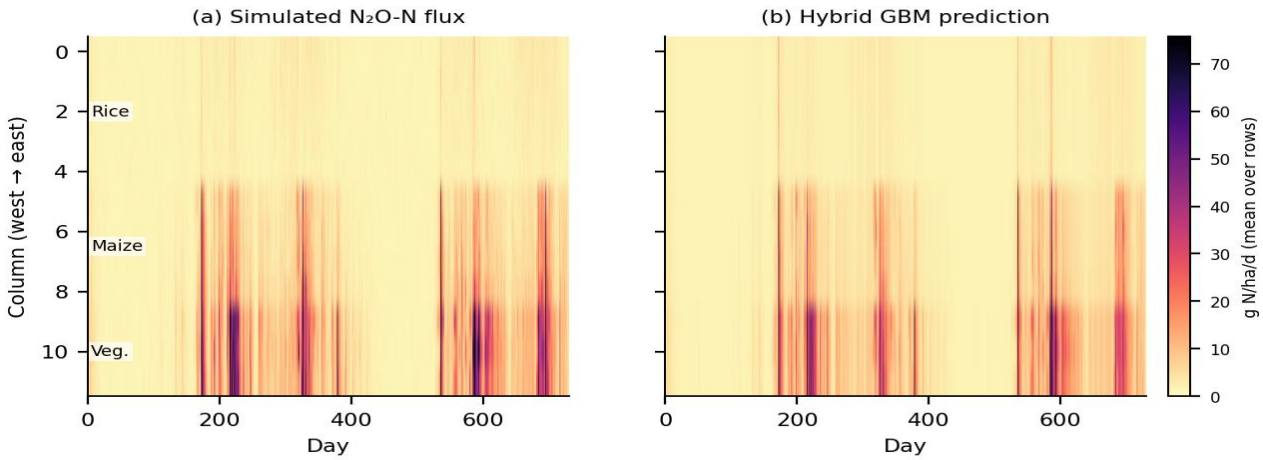


Fig 9. Space–Time View of the N_2O-N Flux Averaged Over Rows (Columns from West to East): (A) Simulated Truth and (B) Hybrid-Model Prediction.

Table 4 show the error of the farm total as a function of the number of chamber parcels and the placement design. With only 6 parcels, random placement gave an RMSE of the farm total of 13 %, against 5 % for stratified and 5 % for covariate-balanced placement, since a random draw can omit a crop system. With 48 parcels the errors were 3.3 %, 3.6 % and 2.3 %. The two coverage-based designs (stratified and covariate-balanced) were similar to each other and clearly better than random placement at 6 parcels, whereas at 12 to 48 parcels the ranking of the three designs changed from size to size (the lowest RMSE was obtained by random placement at 12, stratified at 24 and balanced at 48 parcels), which shows that with five networks per cell these differences are within the sampling noise. Most networks underestimated the total, by 2 to 9 % on average, which reflects the systematic bias of the model rather than the design. In practical terms, a network of a few well-placed parcels that cover every crop and soil class, together with a model, was sufficient to estimate the farm total in this simulation to within about 5 %, but this depends on the CH_4 signal, which is smooth and dominated by one crop, and the farm total of N_2O alone would be more sensitive to the design. Because the cost of a chamber campaign is mostly

labour per sampled day, the results suggest putting the effort into representativeness of parcels and into event-based sampling, rather than into more parcels of the same type.

Table 4. Error of the Estimated Farm-Total CO_2E

Parcels	Random RMSE	Random bias	Stratified RMSE	Stratified bias	Balanced RMSE	Balanced bias
6	13.1	-9.0	5.3	-3.7	5.1	-5.0
12	4.0	-2.8	6.4	-6.3	4.2	-3.4
24	5.5	0.1	3.2	-3.0	4.0	-3.5
48	3.3	-3.3	3.6	-3.5	2.3	-2.0

Management Scenarios

Table 5 compare the management options. In the simulated farm, N_2O represented 33 % of the baseline CO_2e and methane the rest, which sets the order of magnitude of what each option can achieve. Water management in rice was the most effective single measure: AWD reduced the farm CO_2e by 31 % (the 48 % reduction of rice methane partly offset by the assumed N_2O increase) and the yield-scaled emission from 133 to 92 kg CO_2e per tonne of produce. The nitrification inhibitor reduced emissions by 13 %. In contrast, the measures related to the timing and rate of N had small effects on the total: a 20 % lower N rate reduced emissions by 2.4 % at a yield cost of 2 %, forecast-guided timing by 0.6 %, and more split doses changed emissions by 1.0 % (an increase in the simulation, because many smaller applications prolong the period of post-fertilisation sensitivity). The combined package reduced the farm CO_2e by 46 %, with a relative yield of 101.4 % and a yield-scaled emission of 71 kg CO_2e t^{-1}. The ranking would change on a farm where N_2O is a larger share of emissions (for example without rice, or with higher N rates), where N management would be much more important, so that the message is not that N management does not matter but that its importance depends on the farm's emission profile; the share of N_2O-N per hectare was 6 times larger on vegetable parcels than on rice parcels.

The data-driven model reproduced the reduction in the three scenarios that change the management inputs it sees: 3.1 % predicted against 2.4 % true for the lower N rate, 0.2 % against 0.6 % for timing, and 0.7 % against -1.0 % for splitting. All of these differences are within about two percentage points, which is comparable to the bias of the farm total and shows that the model can rank large effects (the 20 % N cut, the inhibitor, AWD) but cannot resolve small ones, and in particular it did not reproduce the sign of the splitting effect. A model trained on baseline data can therefore support counterfactual scenarios only where the changed inputs stay within the range of the training data and the effect is larger than the model's resolution; for the inhibitor and AWD, whose effects are outside the data, external information such as factor multipliers or experiments must be used.

Table 5. Management Scenarios: Farm CO_2E (T/Yr), Reduction from the Baseline in the Simulation (Truth) and Predicted by the Model, Relative Yield and Yield-Scaled Emission

Scenario	Farm CO_2e (t/yr)	Reduction, truth (%)	Reduction, model (%)	Yield (%)	YSE (kg CO_2e/t)
Baseline	413	0.0	0.0	100.0	133
N rate −20 %	403	2.4	3.1	98.0	133
More split doses	417	-1.0	0.7	102.0	132
Forecast-guided timing	410	0.6	0.2	101.5	131
Nitrification inhibitor	359	13.1	12.8	100.0	116
AWD in rice	284	31.1	31.3	100.0	92
Combined package	223	46.0	46.5	101.4	71

Several implications follow for farm management and inventories. First, an accurate farm inventory needs the temporal resolution to capture hot moments and an explicit treatment of flooded rice, which dominated the emissions here; defaults that depend on the crop and the applied N were adequate for ranking the major emitters ($R^2 = 0.80$) but left considerable parcel-level error that the model and kriging removed. Second, the model can direct attention: maps and time series flag the parcels and weeks in which most of the N_2O is emitted, so that measures such as avoiding fertilisation before heavy rain can be targeted. In this simulation the effect of timing on the total was small, but in a farm with more N_2O or with more frequent events it could be larger, and the framework quantifies this. Third, measurement effort should be planned: a handful of parcels that represent the crop and soil strata, with event-based sampling, was enough to constrain the total of this farm. Fourth, remote-sensing covariates such as NDVI and soil moisture provide the spatial and temporal coverage that chambers cannot; in the model the crop and canopy variables contributed about 17 % of the importance. Finally, uncertainty should be reported: the systematic underestimation of the hot moments means that confidence intervals from random error alone would be too narrow.

The principal limitation is that the farm is simulated; the results about accuracy, importance and design depend on assumed mechanisms, noise and a single weather realisation, and real data have additional complications such as chamber artefacts, missing covariates, non-stationary conditions, gaps in sensor data and soil heterogeneity at smaller scales. Only

N_2O and CH_4 were considered, not soil CO_2, soil carbon change or the energy and input emissions that complete a farm footprint. The chamber network was assumed to be known, and the effect of sampling frequency was not varied. The models are not deep-learning sequence models; recurrent or attention-based architectures could use longer histories but need more data, and combining them with process knowledge is an active line of research [12]. Uncertainty was characterised through validation errors and the bias of totals, not through a full probabilistic treatment. The counterfactual scenarios relied on external multipliers for two mitigation measures. Future work will apply the framework to a real farm with continuous (automated chamber or eddy-covariance) data, use satellite radar for flooding and soil moisture, add probabilistic prediction, integrate the model with farm decision tools and extend the analysis to the whole-farm carbon balance.

V. CONCLUSION

This study developed a spatiotemporal, process-guided machine-learning framework for predicting daily, parcel-level nitrous oxide (N_2O) and methane (CH_4) emissions. The framework integrated environmental and management variables with process-model outputs and was evaluated using random, spatial, temporal, and spatiotemporal validation on a simulated farm with known emission fluxes. The hybrid model achieved the best N_2O performance, with an R^2 of 0.27 for unseen parcels in an unseen year, while random forest achieved an R^2 of 0.80 for CH_4. Random validation overestimated N_2O predictive accuracy by a factor of 2.1, highlighting the importance of rigorous validation. Regression kriging improved spatial upscaling, achieving an R^2 of 0.97 for annual CO_2-equivalent emissions on unsampled parcels, although the total farm emissions were underestimated by 5% due to incompletely captured emission peaks. Chamber-network designs covering all crop types and soil classes reduced estimation errors compared with random placement, particularly under limited sampling. Scenario analysis identified rice water management and nitrification inhibitors as the dominant mitigation options, whereas nitrogen-rate reduction and application timing offered smaller benefits. The framework supports spatially explicit emission inventories and data-driven mitigation planning. Future work should validate its performance using measured fluxes from real agricultural farms.

CRediT Author Statement

The authors confirm contribution to the paper as follows:
Conceptualization: Tommy Dalgaard; **Methodology:** Tommy Dalgaard; **Software:** Ketema Niguse Baye and Tommy Dalgaard; **Data Curation:** Ketema Niguse Baye; **Writing- Original Draft Preparation:** Ketema Niguse Baye and Tommy Dalgaard; **Supervision:** Ketema Niguse Baye and Tommy Dalgaard; **Validation:** Ketema Niguse Baye; **Writing-Reviewing and Editing:** Ketema Niguse Baye and Tommy Dalgaard; All authors reviewed the results and approved the final version of the manuscript.

Data Availability

No data was used to support this study.

Conflicts of Interests

The authors declare no conflict of interest.

Funding

No funding agency is associated with this research.

Competing Interests

There are no competing interests.

References

[1]. Z. Xue, "The Emission of Greenhouse Gases from Agricultural Farmland in South Africa: A Review," Open Access Journal of Agricultural Research, vol. 5, no. 2, 2020, doi: 10.23880/oajar-16000246.
[2]. H. Kamyab, M. SaberiKamarposhti, H. Hashim, and M. Yusuf, "Carbon dynamics in agricultural greenhouse gas emissions and removals: a comprehensive review," Carbon Letters, vol. 34, no. 1, pp. 265–289, Dec. 2023, doi: 10.1007/s42823-023-00647-4.
[3]. L. Li, T. Awada, Y. Shi, V. L. Jin, and M. Kaiser, "Global Greenhouse Gas Emissions From Agriculture: Pathways to Sustainable Reductions," Global Change Biology, vol. 31, no. 1, Dec. 2024, doi: 10.1111/gcb.70015.
[4]. X. Xu et al., "Inequality in agricultural greenhouse gas emissions intensity has risen in rural China from 1993 to 2020," Nature Food, vol. 5, no. 11, pp. 916–928, Nov. 2024, doi: 10.1038/s43016-024-01071-1.
[5]. J. Majumdar and J. K. Biswas, "Soil Amendment Strategies for Reducing Greenhouse Gas Emissions from Agricultural Soil," Agricultural Greenhouse Gas Emissions: Problems and Solutions, pp. 81–102, 2024, doi: 10.1007/978-981-97-7554-5_4.
[6]. D. Laborde, A. Mamun, W. Martin, V. Piñeiro, and R. Vos, "Agricultural subsidies and global greenhouse gas emissions," Nature Communications, vol. 12, no. 1, May 2021, doi: 10.1038/s41467-021-22703-1.
[7]. E. H. Bennetzen, P. Smith, and J. R. Porter, "Agricultural production and greenhouse gas emissions from world regions—The major trends over 40 years," Global Environmental Change, vol. 37, pp. 43–55, Mar. 2016, doi: 10.1016/j.gloenvcha.2015.12.004.
[8]. P. Gołasa et al., "Sources of Greenhouse Gas Emissions in Agriculture, with Particular Emphasis on Emissions from Energy Used," Energies, vol. 14, no. 13, p. 3784, Jun. 2021, doi: 10.3390/en14133784.
[9]. C. Guo, X. Liu, and X. He, "A global meta-analysis of crop yield and agricultural greenhouse gas emissions under nitrogen fertilizer application," Science of The Total Environment, vol. 831, p. 154982, Jul. 2022, doi: 10.1016/j.scitotenv.2022.154982.

[10]. K. Jantke, M. J. Hartmann, L. Rasche, B. Blanz, and U. A. Schneider, "Agricultural Greenhouse Gas Emissions: Knowledge and Positions of German Farmers," Land, vol. 9, no. 5, p. 130, Apr. 2020, doi: 10.3390/land9050130.
[11]. Q. Yue, X. Xu, J. Hillier, K. Cheng, and G. Pan, "Mitigating greenhouse gas emissions in agriculture: From farm production to food consumption," Journal of Cleaner Production, vol. 149, pp. 1011–1019, Apr. 2017, doi: 10.1016/j.jclepro.2017.02.172.
[12]. J. Mehmood, M. Shahbaz, J. Wang, and M. N. Malik, "Unveiling the dynamics of agriculture greenhouse gas emissions: The role of energy consumptions and natural resources," Applied Energy, vol. 379, p. 124946, Feb. 2025, doi: 10.1016/j.apenergy.2024.124946.
[13]. C. Maraveas, C.-S. Karavas, D. Loukatos, T. Bartzanas, K. G. Arvanitis, and E. Symeonaki, "Agricultural Greenhouses: Resource Management Technologies and Perspectives for Zero Greenhouse Gas Emissions," Agriculture, vol. 13, no. 7, p. 1464, Jul. 2023, doi: 10.3390/agriculture13071464.
[14]. S. Zhou, B. Liu, J. Wang, D. Jin, and H. Zhang, "Assessing Global Agricultural Greenhouse Gas Emissions: Key Drivers and Mitigation Strategies," Agronomy, vol. 15, no. 6, p. 1336, May 2025, doi: 10.3390/agronomy15061336.
[15]. H. Shao, "Agricultural greenhouse gas emissions, fertilizer consumption, and technological innovation: A comprehensive quantile analysis," Science of The Total Environment, vol. 926, p. 171979, May 2024, doi: 10.1016/j.scitotenv.2024.171979.
[16]. A. Ortiz-Bobea and S. Pieralli, "Unpacking the growth of global agricultural greenhouse gas emissions," Science Advances, vol. 12, no. 3, Jan. 2026, doi: 10.1126/sciadv.aeb8653.
[17]. Y. Han, Q. Tan, T. Zhang, S. Wang, T. Zhang, and S. Zhang, "Development of an assessment-based planting structure optimization model for mitigating agricultural greenhouse gas emissions," Journal of Environmental Management, vol. 349, p. 119322, Jan. 2024, doi: 10.1016/j.jenvman.2023.119322.

Publisher's note: The publisher remains neutral with regard to jurisdictional claims in published maps and institutional affiliations. The content is solely the responsibility of the authors and does not necessarily reflect the views of the publisher.

ISSN: 3104-4654